ADVANCED THEORY AND SIMULATIONS
www.advtheorysimul.com

Combining Both Acceptorless Dehydrogenation and Borrowing Hydrogen Mechanisms in One System as Described by DFT Calculations

*Alessandra Cicolella, Massimo C. D'Alterio, Josep Duran, Sílvia Simon, Giovanni Talarico, and Albert Poater**

The mechanisms for the formation of N-substituted hydrazones by coupling of alcohols and hydrazine, achieved by the sequential processes of acceptorless dehydrogenation and borrowing hydrogen, has been unveiled by density functional theory (DFT) calculations. The release of water and molecular hydrogen as subproducts, combined with the Mn-PNN pincer based catalyst describe a green environment. Mechanistically, apart from describing a complex system of three coupled catalytic pathways, calculations describe the pivotal role of two intermediates, which participate in two catalytic pathways each one. Finally, predictive catalysis plays the role to push forward this reaction toward milder conditions, and thus in line with green chemistry standards.

1. Introduction

The synthesis of N-substituted hydrazones starting from hydrazines and alcohols recently reported by Milstein et al.[1] represents a good example of a successful design of green chemical processes.[2] This reaction is catalyzed by a manganese pincer-based catalyst of type Mn(I)-PNN (see **Scheme 1**) under mild reaction conditions and the reaction pathway was hypothesized as the combination of acceptorless dehydrogenative coupling (ADC) of alcohols and a borrowing hydrogen process (see **Scheme 2**).[3]

Several natural products[4] include N-substituted hydrazones such as NG-061,[5] Leucoagaricone,[6] or Schaefferal A/B,[7] and applications range from serving as chromogens and enhancers of the growth of nerves to building blocks for anticancer drugs, or antifungal, antimicrobial, anti-inflammatory treatments.[8] The usual way[9] to obtain N-substituted hydrazones is the combination of N-substituted hydrazines with aldehydes/ketones whereas the hydrogenation/reduction of azines in heterogeneous systems is a less selective alternative treatment.[10] On the other hand, the combination of Grignard reagents with N_2O is not favored since it leads to poor yields and to the generation of by-products in stoichiometric proportion.[11] As far as concerns the hydrazines, their dehydrogenative coupling with alcohols, instead of hydrazones, first led to deoxygenation by ruthenium,[12] and manganese[13] catalysts in base media, and symmetrical azines by using alcohols and hydrazine were synthesized by a ruthenium pincer complex.[14]

During the last decade, apart from the search of chemicals in catalyzed reactions with high selectivity, most efforts were made to switch from second/third to first row transition metals given their availability, lower prices, and less toxicity.[15] In metal pincer-based catalysts, this basically meant replacing ruthenium and iridium with manganese, iron, cobalt, and nickel. Among them, manganese is the third most abundant metal on earth and has climbed to the top positions, not only for cost, but for low or no toxicity, and variety of applications and selectivity.[16] By using manganese pincer complexes, Michael addition of aliphatic nitriles to α,β-unsaturated carbonyl compounds,[17] and the dehydrogenative coupling of alcohols and imines leading to aldimines,[18] or acrylonitriles[19,20] were obtained as well as a sequence of dehydrogenative reactions,[21,22] or hydrogenations of multiple C-heteroatom bonds and esters.[23,24] Beller et al. provided the C-alkylation of ketones and N-methylation of amines,[25] by combining manganese pincer complexes and hydrogen borrowing protocol,[26] and density functional theory (DFT) calculations rationalized the multiple dehydrogenation steps for the synthesis of amides from alcohols/esters

A. Cicolella, M. C. D'Alterio, J. Duran, S. Simon, A. Poater
Institut de Química Computacional i Catàlisi and Departament de Química
Universitat de Girona
C/ Maria Aurèlia Capmany, 69, Girona, Catalonia 17003, Spain
E-mail: albert.poater@udg.edu
A. Cicolella, G. Talarico
Dipartimento di Scienze Chimiche
Università di Napoli Federico II
Via Cintia, Napoli I-80126, Italy
M. C. D'Alterio
Dipartimento di Chimica e Biologia "A. Zambelli"
Università di Salerno
Via Giovanni Paolo II 132, Fisciano, Salerno 84084, Italy

The ORCID identification number(s) for the author(s) of this article can be found under https://doi.org/10.1002/adts.202100566

Dedicated to Professor Ei-ichi Negishi

DOI: 10.1002/adts.202100566

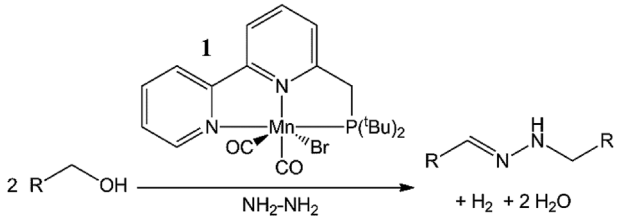

Scheme 1. Reaction of alcohol with hydrazine leading to hydrazone catalyzed by a Mn(I)-PNN complex.

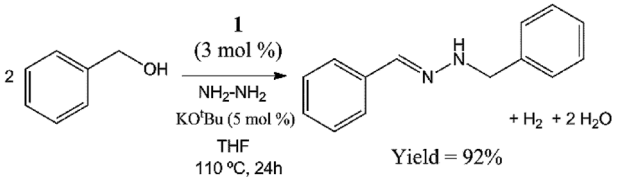

Scheme 3. Experimental details of the studied reaction.

and amines.[27] Experimental works revealed that PNP pincer ligand of the Mn-based catalysts can be modified during the reaction pathway,[28] and computational studies stressed the non-innocent participation of the tridentate ligand metal-pincer based complexes.[29] with their successive aromatization and dearomatization for a series of reaction mechanisms.

Finally, Milstein et al. transformed primary alcohols into alkenes catalyzed by Mn(I)-PNP complexes.[30] Apart from the acceptorless dehydrogenation of the alcohol into aldehyde, the excess of hydrazine led to the formation of hydrazone, and finally producing olefins. The outstanding point is that the (de)protonation of the nitrogen atom of the pincer ligand monitored and guided the two coupled concerted catalytic pathways,[31] whereas for a similar Mn(I)-PNN complex the protonated nitrogen bonded to manganese is stable, and actually favors the reaction of Claisen–Tishchenko condensation by H-bonds with the entering substrates.[32]

With the aim to understand how the ADC and borrowing hydrogen processes coexist, we performed DFT calculations on mechanism(s) leading to the formation of N-substituted hydrazones by mixing alcohols with hydrazine catalyzed by Mn(I)-PNN complex (see Schemes 1 and 2).[1] In an excess of hydrazine, the hydrazone is released together with H_2O and H_2 molecules as the only by-products,[33] revealing the green route of this environmentally friendly protocol.

2. Computational Details

All calculations have been performed by density functional theory (DFT) via the spin-restricted Kohn–Sham (RKS) formalism. DFT calculations were performed using the facilities provided by the Gaussian16 package.[34] For geometry optimization, the GGA-based BP86 functional was used,[35,36] including explicit dispersion corrections to the energy through the Grimme D3BJ method.[37] All geometry optimizations were performed without symmetry constraints in the gas phase. The located stationary points were characterized as minima or transition states by analytical frequency calculations. The split-valence basis set Def2-SVP from Ahlrichs and co-workers was used for all atoms.[38] For single-point energy refinements, the hybrid GGA-based M06 functional was used,[39] with the cc-pVTZ basis set.[40] At this stage, solvent effects were introduced by means of the polarizable continuous solvation model (PCM),[41] using THF as solvent. Gibbs energies were calculated as the sum of the electronic energies at the M06-PCM(THF)/cc-pVTZ//BP86-D3BJ/Def2-SVP level of theory plus the zero-point energies (ZPE) and thermal corrections calculated at the BP86-D3BJ/Def2-SVP computational level in vacuum, at 383 K without translational entropy contributions corrections.[42]

3. Results

The experimental details of the reaction are reported in **Scheme 3**, and starting from the complex **1** (see Scheme 1), the catalytic active species **2** is formed once activated by the base ^{t}BuOK, (see **Figure 1**).

The DFT mechanism(s) reported in Figure 1 are a combination of catalytic cycles. The reaction mechanism was first required to satisfy the dehydrogenation by metal-ligand cooperation (Figure 1, middle catalytic cycle).

Once the benzyl alcohol reacts with the metallic center, its alcoholic proton protonates the methylidyne group of the tridentate ligand on the manganese atom, overcoming a transition state with an associated Gibbs energy barrier of 18.6 kcal mol^{-1}. Next,

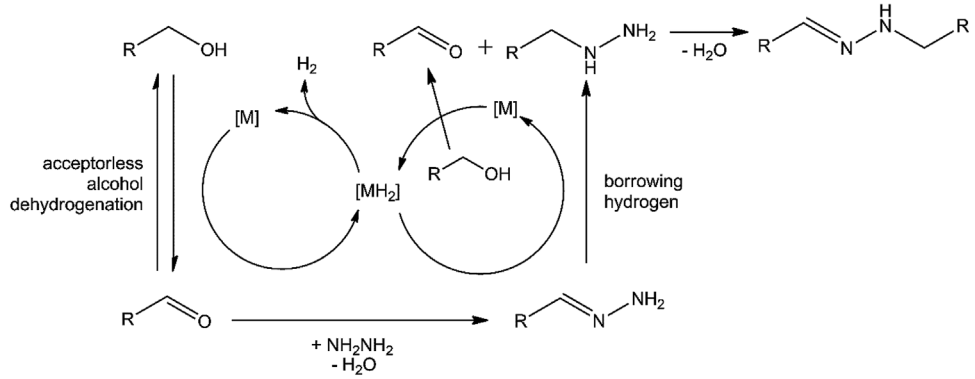

Scheme 2. Proposed mechanisms for the formation of N-substituted hydrazones by coupling alcohols and hydrazine following both acceptorless dehydrogenative coupling and hydrogen borrowing mechanisms in one system.

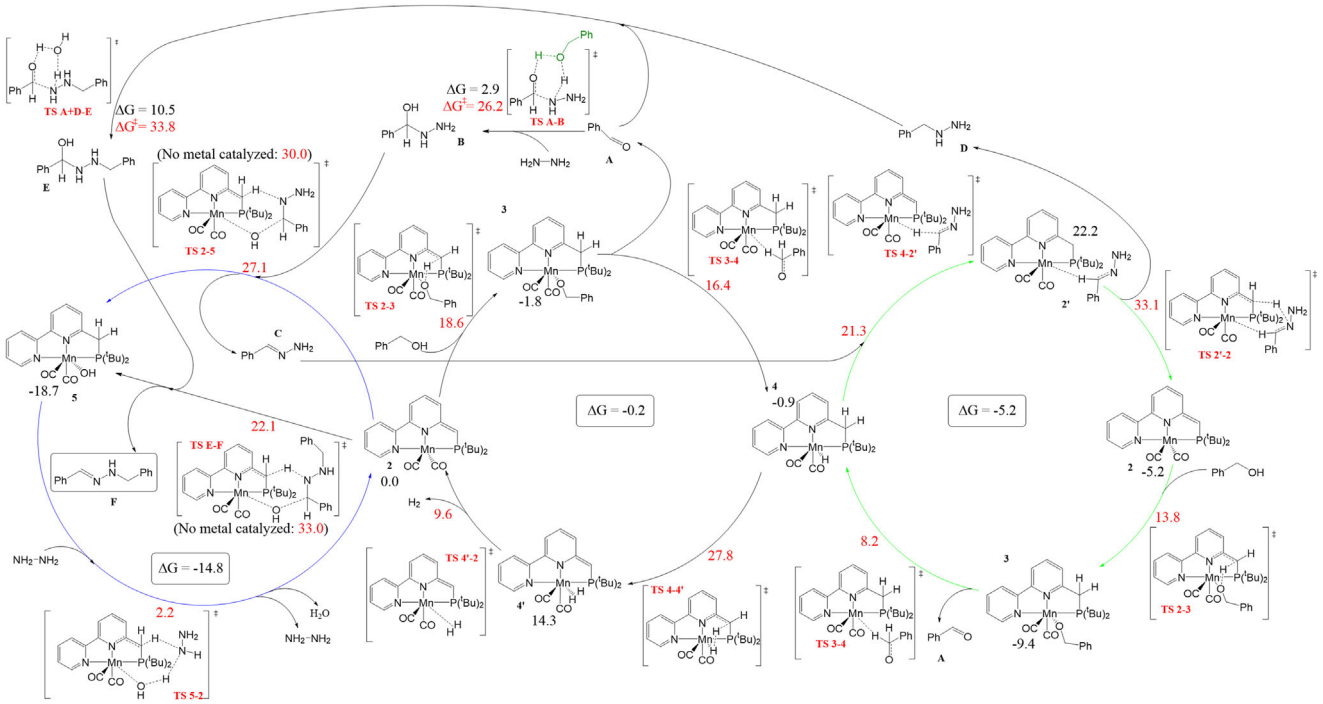

Figure 1. Full reaction mechanism leading to hydrazones (relative Gibbs energies for solvent media in kcal mol^{-1} and referred to catalyst **2**). All data shown were calculated at T = 110 °C, mimicking the experiments.

the formed benzyl oxide ligand of intermediate **3** transfers one hydrogen atom of the methylenic moiety to the metal to get the hydride species **4**, together with the release of the benzaldehyde **A**, overcoming an energy barrier of 18.2 kcal mol^{-1}. From **4** the methylenic moiety of the tridentate ligand deprotonates with an energy barrier of 27.8 kcal mol^{-1} to provide the formation of molecular hydrogen, that then is released to close the catalytic cycle, recovering the catalytic species **2** in a barrierless process.

The formed aldehyde **A** reacts with hydrazine forming the organic molecule **B**, with the assistance of an explicit molecule of benzylic alcohol as a proton shuttle. This non-metal catalyzed is favored neither thermodynamically, that is, endoergonic by 2.9 kcal mol^{-1}, nor kinetically, since it requires to overcome an energy barrier of 26.2 kcal mol^{-1}.[43] From **B**, again the performance of **2** is required, overcoming an energy barrier of 27.1 kcal mol^{-1} (Figure 1, blue catalytic cycle) to facilitate the condensation step. Actually without the interaction by any metal catalyst species the water release as a subproduct is energetically more demanding, up to 30.0 kcal mol^{-1}. In conclusion, in this latter step of condensation **2** behaves as an acceptor, facilitating kinetically a step that is generally presumed to be acceptorless.[20] Furthermore, apart from releasing the hydrazone **C**, it leads to the hydroxylated intermediate **5**, which again has recovered the methylenic arm of the tridentate ligand, and consequently the aromatic character of the pyridine ring.[29,44] Next, this second catalytic cycle is closed with the assistance of an explicit hydrazine molecule that promotes the final release of a water molecule, with an energy barrier of 20.9 kcal mol^{-1} that leads to **2**.

On the other hand, like **2**, **4** also plays a pivotal role, because it does not only participate in the middle catalytic cycle, but in the green one in Figure 1, starting with the formed hydrazone **C** overcoming an overall energy barrier of 33.1 kcal mol^{-1}, to allow the hydrogenation of the double C═N bond to form the corresponding N-substituted hydrazine **D** via a borrowing hydrogen process. This is thanks to both the hydride on the manganese and the closest hydrogen atom of the methylenic moiety of the tridentate ligand on it, with the coordination intermediate **2'** in between. **Figure 2**a displays how important is the H-bond of the former hydride and the metal to fixate the H-transfer from the methylenic group of the pincer ligand to the nitrogen. From **2**, to close this catalytic cycle in green as stated in the first, simply a new benzyl alcohol leads to intermediate **3**, and afterward the benzaldehyde is released to get intermediate **4**. Kinetically the two steps require to overcome an overall energy barrier of 19.0 kcal mol^{-1}.

The hydrazine **D** assisted by a water molecule and the interaction of a second benzaldehyde achieves the hydrazone **E**, with a kinetic cost of 33.8 kcal mol^{-1} and a relative unfavored thermodynamics of 10.5 kcal mol^{-1}, without any assistance of the metal catalyst. It is worth to note that this step is assisted by a water molecule (see Figure 2b), whereas with an explicit molecule of benzyl alcohol requires just the additional kinetic energy amount of 0.3 kcal mol. However, next **E** dehydrogenates thanks to the interaction with the catalytic species **2** that transforms into intermediate **5**, as part of an additional reaction of the catalytic cycle in blue in Figure 1.

The rate determining step (rds) corresponds to the **2**—**2'** step,[45] and consists of the formation of the hydrazine intermediate **D**, hydrogenating the former hydrazone **C**, even though microkinetic studies might help to confirm the nature of this rds.[46] In addition, any overestimation of the entropy was further explored with the model of Martin et al,[47] and further evaluated

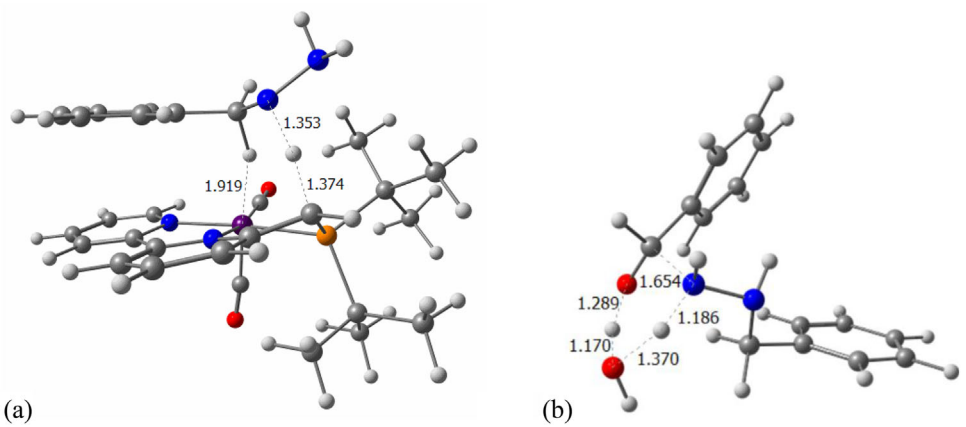

Figure 2. Transition states a) **2′-2** and b) **A+D-E** (assisted by water); selected distances given in Å.

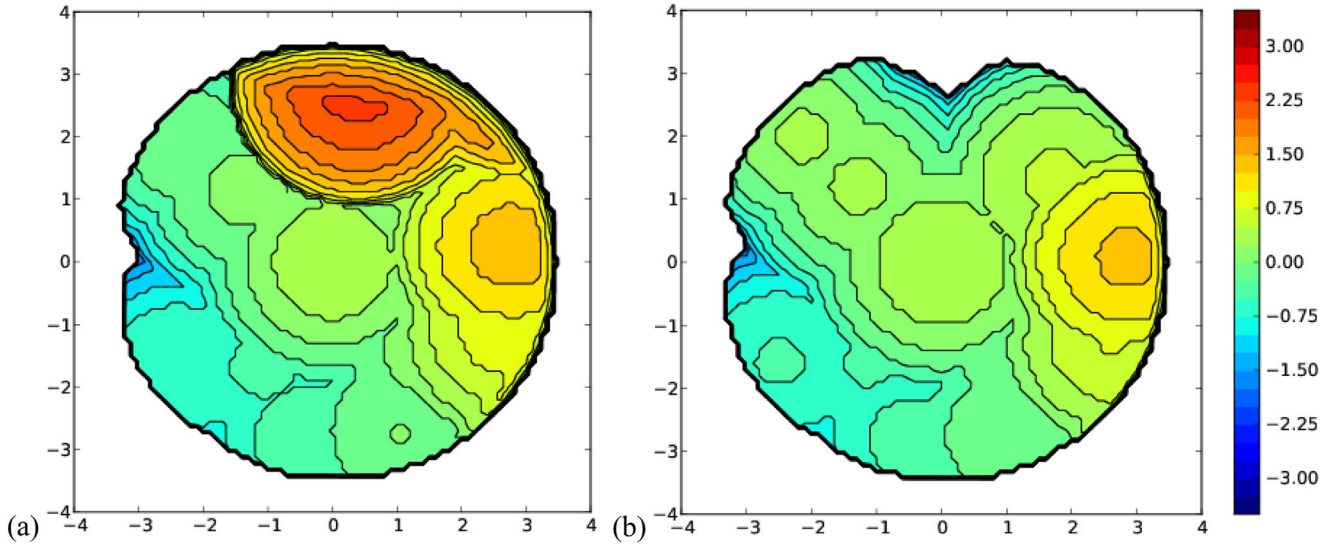

Figure 3. a) Steric maps (plane *xy*) of the transition state 2′-2, with ^{t}Bu and b) hydrogen substituents on the phosphorous atom. $\%V_{Bur}$ is the percent of buried volume. The manganese atom is at the origin and the H transferred to the metal is on the *z*-axis, whereas the other transferred H atom is on the *x*-axis. The isocontour curves of the steric maps are given in Å.

and applied by Cavallo et al,[48] but no significant difference was confirmed. Following the strategy of predictive catalysis, the substitution of the ^{t}Bu groups on the phosphorous atoms of the catalyst modifies the energy barrier of the rds. The energy barrier of 34.0 kcal mol^{-1} increases by just 0.3 kcal mol^{-1} with the trifluoromethyl groups, while it drops 4.2, 2.4, and 1.4 kcal mol^{-1} with H, F, and the methoxy ligands, respectively. To go deeper into the sterical hindrance induced by the groups on the phosphorous atom, the SambVca2.1 package to generate the steric maps developed by Cavallo and co-workers was used.[49] The plane to evaluate the reactivity including both H atoms that are transferred from hydrazine **C** to **D** was used as a reference. The overall $\%V_{Bur}$ values are 59.6%, 52.2%, 56.1%, 53.5%, and 54.4%, whereas for the particular quadrant affected by the phosphorous atom and its substituents 77.4%, 58.1%, 71.7%, 48.7%, and 42.4% for the experimentally tested ^{t}Bu and the in silico H, OCH_3, F, and CF_3 groups, respectively. Steric maps displayed in **Figure 3** clarify the huge difference in the quadrant where the substituents on the phosphorous atom are accommodated when substituting the ^{t}Bu substituents by simple H atoms (see the Supporting Information for the other steric maps).[24,50] Thus, the low hindered systems tend to favor the kinetics for the rds, and thus, sterically, the highly hindered ^{t}Bu group is not the perfect substituent on the phosphorous atom. This confirms that the higher sterical hindrance on the phosphine does not support the catalytic reaction comparing the hydrogen atom with the ^{t}Bu group,[51] whereas electronically, electrodonating groups favor the reaction, comparing CF_3 with OCH_3, or also F with H.

Even though quantitatively the sterics dominate with respect to the electronics, the hydrogen substituents are experimentally difficult to bond to phosphorous, while methoxy ligands are somewhat more facile to introduce, together with the phosphorous labeled as phosphites, and previously yet found more reactive than phosphines, when directly compared.[52] In addition,

the terminal NH_2 moiety is able to create a H-bond of 2.152 Å with ^{t}Bu groups on the P atoms (see Figure 2a), whereas much weaker but still strong,[53] elongated to 2.699 Å with hydrogens as substituents. On the other hand, the methoxy ligands lead to a stronger H-bond of 2.048 Å, not a N···H interaction, but an O···H interaction. To sum up, considering the results for the less sterically hindered system, with just hydrogens on the P atoms, these H-bonds do not manage the kinetics, but the heteroatoms of the substituting groups.

4. Conclusions

DFT calculations have unveiled the mechanism(s) of the manganese catalyzed coupling of alcohols with hydrazine that combines the borrowing hydrogen and acceptorless dehydrogenation in one system giving as a result N-substituted hydrazones together with water and molecular hydrogen. The complex reaction pathway is a combination of three catalytic pathways that are linked not only by two metal catalyst species that have a pivotal role, but also the organic subproducts that are released from them are fundamental for the other catalytic pathways.

As synthetically designed, it is a sustainable reaction, and with relative mild conditions. Here the rds was found out, and by predictive catalysis in a humble way the strategy proposed by calculations was simply the modification of the substituents on the P atoms of the pincer ligand. The most rational combination leads to the hypothesis that the exchange of phosphines by phosphites is the most facile modification of the metal catalyst. Nevertheless, the margin is not that high since a non-metal catalyzed step is in close competition.

Supporting Information

Supporting Information is available from the Wiley Online Library or from the author.

Acknowledgements

A.P. is a Serra Húnter Fellow and ICREA Academia Prize 2019. S.S. and A.P. thank the Spanish MINECO for projects and PID2020-13711GB-I00 and PGC2018-097722-B-I00. The authors thank Dr. L. M. Azofra for helpful comments.

Conflict of Interest

The authors declare no conflict of interest.

Data Availability Statement

The data that support the findings of this study are available in the supplementary material of this article.

Keywords

acceptorless dehydrogenative coupling, borrowing hydrogen, manganese, pincer ligands

Received: November 30, 2021
Revised: March 5, 2022
Published online: April 12, 2022

[1] U. K. Das, Y. Ben-David, Y. Diskin-Posner, D. Milstein, *Angew. Chem., Int. Ed.* **2018**, *57*, 2179.
[2] P. Nad, A. Mukherjee, *Asian J. Org. Chem.* **2021**, *10*, 1958.
[3] R. Fertig, T. Irrgang, F. Freitag, J. Zander, R. Kempe, *ACS Catal.* **2018**, *8*, 8525.
[4] G. Le Goff, J. Ouazzani, *Bioorg. Med. Chem.* **2014**, *22*, 6529.
[5] M. Ito, N. Sakai, K. Ito, F. Mizobe, K. Hanada, K. Mizoue, R. Bhandari, T. Eguchi, K. J. Kakinuma, *J. Antibiot.* **1999**, *52*, 224.
[6] S. Hilbig, T. Andries, W. Steglich, T. Anke, *Angew. Chem., Int. Ed.* **1985**, *24*, 1063.
[7] R. Kileci-Ksoll, C. Winklhofer, W. Steglich, *Synthesis* **2010**, *13*, 2287.
[8] a) S. Rollas, G. Kucukguzel, *Molecules* **2007**, *12*, 1910; b) R. Narang, B. Narasimhan, S. Sharma, *Curr. Med. Chem.* **2012**, *19*, 569; c) M. S. Abdelfattah, K. Toume, M. A. Arai, H. Masu, M. Ishibashi, *Tetrahedron Lett.* **2012**, *53*, 3346; d) M. S. Abdelfattah, K. Toume, M. Ishibashi, *J. Antibiot.* **2012**, *65*, 245.
[9] a) T. Imai, R. Harigae, K. Moriyama, H. Togo, *J. Org. Chem.* **2016**, *81*, 3975; b) Z. H. Shang, Q. Q. Chua, S. Tan, *Synthesis* **2015**, *47*, 1032.
[10] a) H. H. Fox, J. T. Gibas, *J. Org. Chem.* **1955**, *20*, 60; b) J. M. Khurana, B. M. Kandpal, P. Sharma, M. Gupta, *Monatsh. Chem.* **2015**, *146*, 187; c) E. Charistoudi, M. G. Kallitsakis, I. Charisteidis, K. S. Triantafyllidis, I. N. Lykakisa, *Adv. Synth. Catal.* **2017**, *359*, 2949.
[11] A. G. Tskhovrebov, R. Scopelliti, K. Severin, *Organometallics* **2014**, *33*, 2405.
[12] X.- J. Dai, C.- J. Li, *J. Am. Chem. Soc.* **2016**, *138*, 5433.
[13] J. O. Bauer, S. Chakraborty, D. Milstein, *ACS Catal.* **2017**, *7*, 4462.
[14] J. O. Bauer, G. Leitus, Y. Ben-David, D. Milstein, *ACS Catal.* **2016**, *6*, 8415.
[15] a) B. Maji, M. K. Barman, *Synthesis* **2017**, *49*, 3377; b) F. Kallmeier, R. Kempe, *Angew. Chem., Int. Ed.* **2018**, *57*, 46; c) R. M. C. Bullock, *Science* **2013**, *342*, 1054; d) S. Z. Tasker, A. Eric, E. A. Standley, T. F. Jamison, *Nature* **2014**, *509*, 299; e) B. Su, Z.-C. Cao, Z.-J. Shi, *Acc. Chem. Res.* **2015**, *48*, 886; f) T. Zell, D. Milstein, *Acc. Chem. Res.* **2015**, *48*, 1979; g) P. Chirik, M. Morris, *Acc. Chem. Res.* **2015**, *48*, 2495.
[16] a) M. Garbe, K. Junge, M. Beller, *Eur. J. Org. Chem.* **2017**, 4344; b) A. Mukherjee, D. Milstein, *ACS Catal.* **2018**, *8*, 11435; c) J. R. Carney, B. R. Dillon, S. P. Thomas, *Eur. J. Org. Chem.* **2016**, *2016*, 3912; d) V. Zubar, Y. Lebedev, L. M. Azofra, L. Cavallo, O. El-Sepelgy, M. Rueping, *Angew. Chem., Int. Ed.* **2018**, *57*, 13439; e) A. Brzozowska, L. M. Azofra, V. Zubar, I. Atodiresei, L. Cavallo, M. Rueping, O. El-Sepelgy, *ACS Catal.* **2018**, *8*, 4103; f) S. Weber, B. Stöger, K. Kirchner, *Org. Lett.* **2018**, *20*, 7212; g) N. Biswas, K. Das, B. Sardar, D. Srimani, *Dalton Trans.* **2019**, *48*, 6501; h) J. C. Borghs, M. A. Tran, J. Sklyaruk, M. Rueping, O. El-Sepelgy, *J. Org. Chem.* **2019**, *84*, 7927; i) A. Nodzewska, A. Wadolowska, M. Watkinson, *Coord. Chem. Rev.* **2019**, *382*, 181.
[17] A. Nerush, M. Vogt, U. Gellrich, G. Leitus, Y. Ben-David, D. Milstein, *J. Am. Chem. Soc.* **2016**, *138*, 6985.
[18] a) A. Mukherjee, A. Nerush, G. Leitus, L. J. W. Shimon, Y. Ben David, N. A. Jalapa, D. Milstein, *J. Am. Chem. Soc.* **2016**, *138*, 4298; b) J. Masdemont, J. A. Luque-Urrutia, M. Gimferrer, D. Milstein, A. Poater, *ACS Catal.* **2019**, *9*, 1662.
[19] S. Chakraborty, U. K. Das, Y. Ben-David, D. Milstein, *J. Am. Chem. Soc.* **2017**, *139*, 11710.
[20] J. A. Luque-Urrutia, M. Solà, D. Milstein, A. Poater, *J. Am. Chem. Soc.* **2019**, *141*, 2398.
[21] a) N. A. Espinosa-Jalapa, A. Kumar, Y. Diskin-Posner, G. Leitus, D. Milstein, *J. Am. Chem. Soc.* **2017**, *139*, 11722; b) S. Fu, Z. Shao, Y. Wang, Q. Liu, *J. Am. Chem. Soc.* **2017**, *139*, 11941; c) M. Mastalir, E. Pittenauer, G. Allmaier, K. Kirchner, *J. Am. Chem. Soc.* **2017**, *139*, 8812; d) S. Chakraborty, U. Gellrich, Y. Diskin-Posner, G. Leitus, L. Avram, D. Milstein, *Angew. Chem., Int. Ed.* **2017**, *56*, 4229; e) N. Deibl, R. Kempe, *Angew. Chem., Int. Ed.* **2017**, *56*, 1663.

[22] a) G.-Y. Zhang, T. Irrgang, T. Dietel, F. Kallmeier, R. Kempe, *Angew. Chem., Int. Ed.* **2018**, *57*, 9131; b) S. P. Midya, J. Pitchaimani, V. G. Landge, V. Madhu, E. Balaraman, *Catal. Sci. Technol.* **2018**, *8*, 3469; c) P. Gao, J. Zhang, *Adv. Theory Simul.* **2020**, *3*, 2000139.
[23] a) F. Kallmeier, T. Irrgang, T. Dietel, R. Kempe, *Angew. Chem., Int. Ed.* **2016**, *55*, 11806; b) S. Elangovan, C. Topf, S. Fischer, H. Jiao, A. Spannenberg, W. Baumann, R. Ludwig, K. Junge, M. Beller, *J. Am. Chem. Soc.* **2016**, *138*, 8809; c) N. A. Espinosa-Jalapa, A. Nerush, L. J. W. Shimon, G. Leitus, L. Avram, Y. Ben-David, D. Milstein, *Chem. Eur. J.* **2017**, *23*, 5934; d) S. Elangovan, M. Garbe, H. Jiao, A. Spannenberg, K. Junge, M. Beller, *Angew. Chem., Int. Ed.* **2016**, *55*, 15364; e) V. Papa, J. R. Cabrero-Antonino, E. Alberico, A. Spanneberg, K. Junge, H. Junge, M. Beller, *Chem. Sci.* **2017**, *8*, 3576.
[24] a) J. A. Luque-Urrutia, A. Poater, *Inorg. Chem.* **2017**, *56*, 14383; b) M. Tomasini, J. Duran, S. Simon, L. M. Azofra, A. Poater, *Mol. Catal.* **2021**, *510*, 111692.
[25] a) M. Peña-López, P. Piehl, S. Elangovan, H. Neumann, M. Beller, *Angew. Chem., Int. Ed.* **2016**, *55*, 14967; b) S. Elangovan, J. Neumann, J.-B. Sortais, K. Junge, C. Darcel, M. Beller, *Nat. Commun.* **2016**, *7*, 12641.
[26] a) M. H. S. A. Hamid, P. A. Slatford, J. M. J. Williams, *Adv. Synth. Catal.* **2007**, *349*, 1555; b) C. Gunanathan, D. Milstein, *Angew. Chem., Int. Ed.* **2008**, *47*, 8661; c) M. H. S. A. Hamid, C. L. Allen, G. W. Lamb, A. C. Maxwell, H. C. Maytum, A. J. A. Watson, J. M. J. Williams, *J. Am. Chem. Soc.* **2009**, *131*, 1766; d) Y. Obora, *ACS Catal.* **2014**, *4*, 3972.
[27] a) A. Kumar, N. A. Espinosa-Jalapa, G. Leitus, Y. Diskin-Posner, L. Avram, D. Milstein, *Angew. Chem., Int. Ed.* **2017**, *56*, 14992; b) J. A. Luque-Urrutia, T. Pèlachs, M. Solà, A. Poater, *ACS Catal.* **2021**, *11*, 6155.
[28] M. Mastalir, M. Glatz, N. Gorgas, B. Stöger, E. Pittenauer, G. Allmaier, L. F. Veiros, K. Kirchner, *Chem. Eur. J.* **2016**, *22*, 12316.
[29] a) T. P. Gonçalves, K.-W. Huang, *J. Am. Chem. Soc.* **2017**, *139*, 13442; b) H. Li, T. P. Gonçalves, D. Lupp, K.-W. Huang, *ACS Catal.* **2019**, *9*, 1619.
[30] U. K. Das, S. Chakraborty, Y. Diskin-Posner, D. Milstein, *Angew. Chem., Int. Ed.* **2018**, *57*, 13444.
[31] L. M. Azofra, A. Poater, *Dalton Trans.* **2019**, *48*, 14122.
[32] L. M. Azofra, L. Cavallo, *Theor. Chem. Acc.* **2019**, *138*, 64.
[33] a) B. Mei, G. Mul, B. Seger, *Adv. Sustainable Syst.* **2017**, *1*, 1600035; b) P. Cendula, A. Sancheti, P. Simon, *Adv. Theory Simul.* **2021**, *4*, 2100312.
[34] M. J. Frisch, G. W. Trucks, H. B. Schlegel, G. E. Scuseria, M. A. Robb, J. R. Cheeseman, G. Scalmani, V. Barone, B. Mennucci, G. A. Petersson, H. Nakatsuji, M. Caricato, X. Li, H. P. Hratchian, A. F. Izmaylov, J. Bloino, G. Zheng, J. L. Sonnenberg, M. Hada, M. Ehara, K. Toyota, R. Fukuda, J. Hasegawa, M. Ishida, T. Nakajima, Y. Honda, O. Kitao, H. Nakai, T. Vreven, J. A. Montgomery Jr., et al., Gaussian 09, Revision E.01, Gaussian, Inc., Wallingford CT, **2009**.
[35] A. Becke, *Phys. Rev. A* **1988**, *38*, 3098.
[36] a) J. P. Perdew, *Phys. Rev. B* **1986**, *33*, 8822; b) J. P. Perdew, *Phys. Rev. B* **1986**, *34*, 7406.
[37] a) S. Grimme, J. Antony, S. Ehrlich, H. Krieg, *J. Chem. Phys.* **2010**, *132*, 154104; b) S. Grimme, S. Ehrlich, L. Goerigk, *J. Comput. Chem.* **2011**, *32*, 1456; c) E. R. Johnson, A. D. Becke, *J. Chem. Phys.* **2006**, *124*, 174104.
[38] A. Schäfer, H. Horn, R. Ahlrichs, *J. Chem. Phys.* **1992**, *97*, 2571.
[39] Y. Zhao, D. G. Truhlar, *Theor. Chem. Acc.* **2008**, *120*, 215.
[40] R. A. Kendall, T. H. Dunning Jr., R. J. Harrison, *J. Chem. Phys.* **1992**, *96*, 6796.
[41] J. Tomasi, M. Persico, *Chem. Rev.* **1994**, *94*, 2027.
[42] V. Barone, G. Talarico, *Mol. Catal.* **2018**, *452*, 138.
[43] W. M. Dagnaw, Y. Lu, R.-H. Zhao, Z.-X. Wang, *Organometallics* **2019**, *38*, 3590.
[44] S. Escayola, M. Solà, A. Poater, *Inorg. Chem.* **2020**, *59*, 9374.
[45] S. Kozuch, S. Shaik, *Acc. Chem. Res.* **2011**, *44*, 101.
[46] C. D.-T. Nielsen, J. Burés, *Chem. Sci.* **2019**, *10*, 348.
[47] R. L. Martin, P. J. Hay, L. R. Pratt, *J. Phys. Chem. A* **1998**, *102*, 3565.
[48] a) A. Poater, E. Pump, S. V. C. Vummaleti, L. Cavallo, *J. Chem. Theory Comput.* **2014**, *10*, 4442; b) S. Manzini, A. Poater, D. J. Nelson, L. Cavallo, A. M. Z. Slawin, S. P. Nolan, *Angew. Chem., Int. Ed.* **2014**, *53*, 8995; c) Y. Minenkov, E. Chermak, L. Cavallo, *J. Chem. Theory Comput.* **2016**, *12*, 1542; d) A. Gómez-Suárez, Y. Oonishi, A. R. Martin, S. V. C. Vummaleti, D. J. Nelson, D. B. Cordes, A. M. Z. Slawin, L. Cavallo, S. P. Nolan, A. Poater, *Chem. Eur. J.* **2016**, *22*, 1125.
[49] a) L. Falivene, R. Credendino, A. Poater, A. Petta, L. Serra, R. Oliva, V. Scarano, L. Cavallo, *Organometallics* **2016**, *35*, 2286, b) L. Falivene, Z. Cao, A. Petta, L. Serra, A. Poater, R. Oliva, V. Scarano, L. Cavallo, *Nat. Chem.* **2019**, *11*, 872.
[50] a) M. Gimferrer, Y. Minami, Y. Noguchi, T. Hiyama, A. Poater, *Organometallics* **2018**, *37*, 1456; b) R. Mariz, A. Poater, M. Gatti, E. Drinkel, J. J. Bürgi, X. Luan, S. Blumentritt, A. Linden, L. Cavallo, R. Dorta, *Chem. Eur. J.* **2010**, *16*, 14335; c) A. Poater, L. Cavallo, *Dalton Trans.* **2009**, *41*, 8878; d) M. Rouen, P. Queval, E. Borré, L. Falivene, A. Poater, M. Berthod, F. Hugues, L. Cavallo, O. Baslé, H. Olivier-Bourbigou, M. Mauduit, *ACS Catal.* **2016**, *6*, 7970.
[51] S. Dehghani, S. Sadjadi, N. Bahri-Laleh, M. Nekoomanesh-Haghighi, A. Poater, *Appl. Organomet. Chem.* **2019**, *33*, e4891.
[52] a) X. Bantreil, A. Poater, C. A. Urbina-Blanco, Y. D. Bidal, L. Falivene, R. A. M. Randall, L. Cavallo, A. M. Z. Slawin, C. S. J. Cazin, *Organometallics* **2012**, *31*, 7415; b) Y. D. Bidal, C. A. Urbina-Blanco, A. Poater, D. B. Cordes, A. M. Z. Slawin, L. Cavallo, C. S. J. Cazin, *Dalton Trans.* **2019**, *48*, 11326.
[53] G. Gilli, P. Gilli, *J. Mol. Struct.* **2000**, *552*, 1.